

Effect of combined ion and electron irradiation on 2 eV luminescence band in hexagonal boron nitride

© Yu.V. Petrov,^{1,*} O.A. Gogina,¹ O.F. Vyvenko,¹ K. Bolotin,² S. Kovalchuk²

¹ Faculty of physics, Saint-Petersburg state university,
199034 Saint-Petersburg, Russia

² Department of Physics, Freie Universität Berlin,
14195 Berlin, Germany

*e-mail: y.petrov@spbu.ru

Point defects in wide-bandgap semiconductors, in particular in hexagonal boron nitride, are promising candidates for single-photon emitters, used in quantum informatics. The cathodoluminescence of ion beam induced defects in hexagonal boron nitride, as well as the effect of prolonged electron irradiation on the intensity of the luminescence was investigated. It has been shown that upon the ion irradiation the intensity of both band-to-band emission and defect related emission decreased, and during subsequent electron irradiation the intensity of 2 eV luminescence band increased, whereas the intensity of other bands remained unchanged.

Keywords: cathodoluminescence, ion beam irradiation, electron beam irradiation, hexagonal boron nitride

DOI: 10.61011/TP.2023.07.56627.62-23

Introduction

Nowadays one of the most important research directions of quantum cryptography is the development of single photon emitters, which can be different quantum systems, including point defects in semiconductors [1], such as NV-centers in diamond [2]. Hexagonal boron nitride (h-BN) is a promising wide-bandgap semiconductor [3], with indirect band gap of 6.08 eV [4], which possesses several luminescence bands in visible and near ultraviolet range [5]. The most investigated luminescence bands of this material are bands centered at 650 nm (1.9 eV), 320 nm (3.9 eV) and 215 nm (5.8 eV). The 5.8 eV band is close to the material fundamental absorption edge and, according to [4], can be attributed to the indirect exciton. Regarding the other two luminescence bands, the nature and the creation conditions of the corresponding luminescence centers are still under discussion. So, as a rule, the defect responsible for 3.9 eV luminescence band is attributed to the presence of carbon impurity [3], whereas some existing data indicate that it might include oxygen as well [6], and 1.9 eV band is attributed to quite diverse intrinsic defects which might be a nitrogen vacancy or complexes of vacancies with antisites and impurities [5].

The development of abovementioned single photon sources requires the control of the concentration of the desirable point defects, at that the local action onto luminescence properties of the material is of the main interest for application of the created structures. In this connection, several efforts to form centers of radiative and non-radiative recombination in hexagonal boron nitride have been made utilizing the irradiation with ions [7–11], electrons [3,12,13], neutrons [14] and laser irradiation [12] as well as electron beam induced local deposition of carbon [15]. At the same time, the processes of defect formation under the treatments listed above are not sufficiently studied, so the available published data are sometimes discrepant.

Recently we have found [10] that in addition to the decrease of band-to-band emission as a result of local helium ion irradiation, at certain ion fluence it is possible to achieve the enhancement of the intensity of the 1.9 eV luminescence band. Further investigations revealed that the intensity of that band in the samples previously irradiated with helium ions enlarged after prolonged electron beam exposure [16].

This paper presents the results of more detailed investigation of the effect of sequential irradiation of hexagonal boron nitride with focused beams of helium ions and electrons on the intensity of 1.9 eV cathodoluminescence (CL) band. It was found that electron irradiation of areas previously irradiated with ions at various fluences, gave rise to a non-monotonic variation of the intensity of 1.9 eV band so, that the final CL signal level exceeded the initial one from non-irradiated sample, which turn out to be non-sensitive to the electron irradiation.

1. Experimental methods

Thin h-BN monocrystal obtained by exfoliation from bulk crystal grown at high temperature and pressure from barium solution [17] and transferred onto Si₃N₄/Si substrate was investigated in this study. The thickness of the sample was determined with atomic force microscopy (AFM) and was found to be 175 nm.

Local irradiation with the focused helium ion beam was performed utilizing the helium ion microscope Zeiss Orion Plus with ion energy of 30 keV and ion fluences ranging from $5 \cdot 10^{13}$ to $3.2 \cdot 10^{15}$ cm⁻². $3 \times 25 \mu\text{m}$ rectangular areas separated from each other by $1 \mu\text{m}$ space were irradiated in a scanning mode at different fluences with 3 nm scan step that is small enough to provide homogeneous ion flux over the entire area [16].

Cathodoluminescence measurements were performed with scanning electron microscope (SEM) Zeiss SUPRA 40VP, equipped with CL detection Gatan

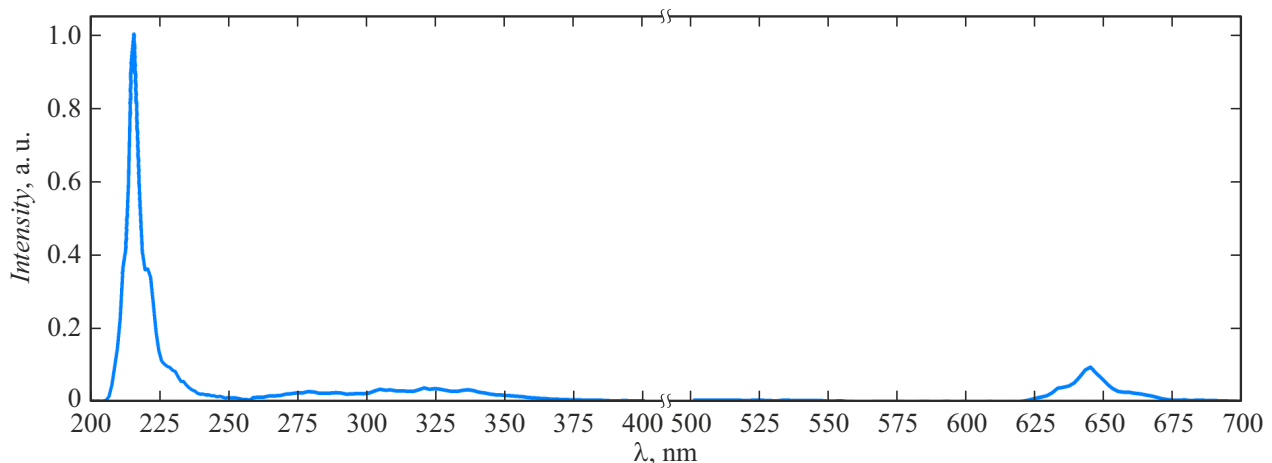


Figure 1. CL spectrum of the pristine h-BN sample normalized by maximum intensity.

Mono CL3+. The spectra were recorded in continuous scanning mode in wavelength range from 200 to 700 nm under the electron excitation with an energy of 5 keV and the beam current of 3 nA.

CL maps were acquired both with monochromator and with bandpass filter with the bandwidth of 80 nm, to avoid the overlay of the second order diffraction from the shorter wavelength bands. Total electron fluence during map acquisition was $7.6 \cdot 10^{16} \text{ cm}^{-2}$.

The measurements of time dependence of CL intensity under the electron irradiation was performed with bandpass filter with the bandwidth of 80 nm during continuous scanning of $1 \times 1 \mu\text{m}$ square with the electron current density of $1.9 \cdot 10^{18} \text{ cm}^{-2} \cdot \text{c}^{-1}$.

2. Experimental results

Typical CL spectrum of the hexagonal boron nitride sample recorded from non-irradiated area of the sample is shown in Fig. 1. The spectrum contains an intense band peaked at 215 nm, a weak broad band centered at 320 nm and the band at 640 nm.

SEM image and monochromatic CL maps at different wavelengths are shown in Fig. 2 both for pristine sample and for helium ion irradiated sample. As one can see from Fig. 2, *b*, CL intensity at 215 nm wavelength was distributed almost uniformly over the sample area, decreasing at elongated structures, some of which coincide with the sample morphology peculiarities, observed in SEM image (Fig. 2, *a*). At the same elongated features the CL intensity enhancement of 320 nm band (Fig. 2, *c*) and of 640 nm band (Fig. 2, *d*) was observed. Besides that, the lower CL intensity of these two bands was observed in the rest area of the sample.

CL maps acquired at 215 nm and 320 nm revealed a decrease of the intensity in the helium ion irradiated areas for all ion fluences (Fig. 2, *f–g*). In the case of 640 nm band, the intensity decrease was observed mostly pronounced

in elongated structures, which were brightest before the irradiation.

The kinetics of the intensity of 640 nm band during electron irradiation were measured in ion irradiated areas. Respective time dependencies of the intensity are depicted in Fig. 3.

As one can see from the figure, during electron irradiation the CL intensity in 640 nm band first increased fast and then decreased slowly, and the time constants of the intensity rise and decay depended on helium ion fluence. In the case of pristine sample, no intensity growth was observed within experimental error. Maximum intensity of 640 nm CL band observed after prolonged electron irradiation for all ion irradiated areas exceeded the intensity of the same CL band in pristine sample.

CL maps, acquired after the measurements of CL intensity kinetics, are shown in Fig. 4. The map acquired at 640 nm (Fig. 4, *c*) revealed the increase of the intensity in electron irradiated areas. For the other wavelengths no intensity enhancement was observed.

Electron irradiation of ion irradiated areas resulted in formation of the layer of non-volatile compounds, deposited from residual gases. The thickness of such layer was inhomogeneous across electron irradiated area, being the largest at the edges and decreasing in the center. AFM measurements showed that maximum thickness of the deposited layers varied from 7 to 10 nm and was proportional to the total time of electron beam irradiation. No dependence of the thickness of deposited layer on helium ion irradiation fluence was found within the experimental error.

Discussion

CL bands, observed in the spectrum, correspond to the characteristic luminescence bands of hexagonal boron nitride previously observed by other authors [3–6]. As one can see from CL maps (Fig. 2), helium ion irradiation

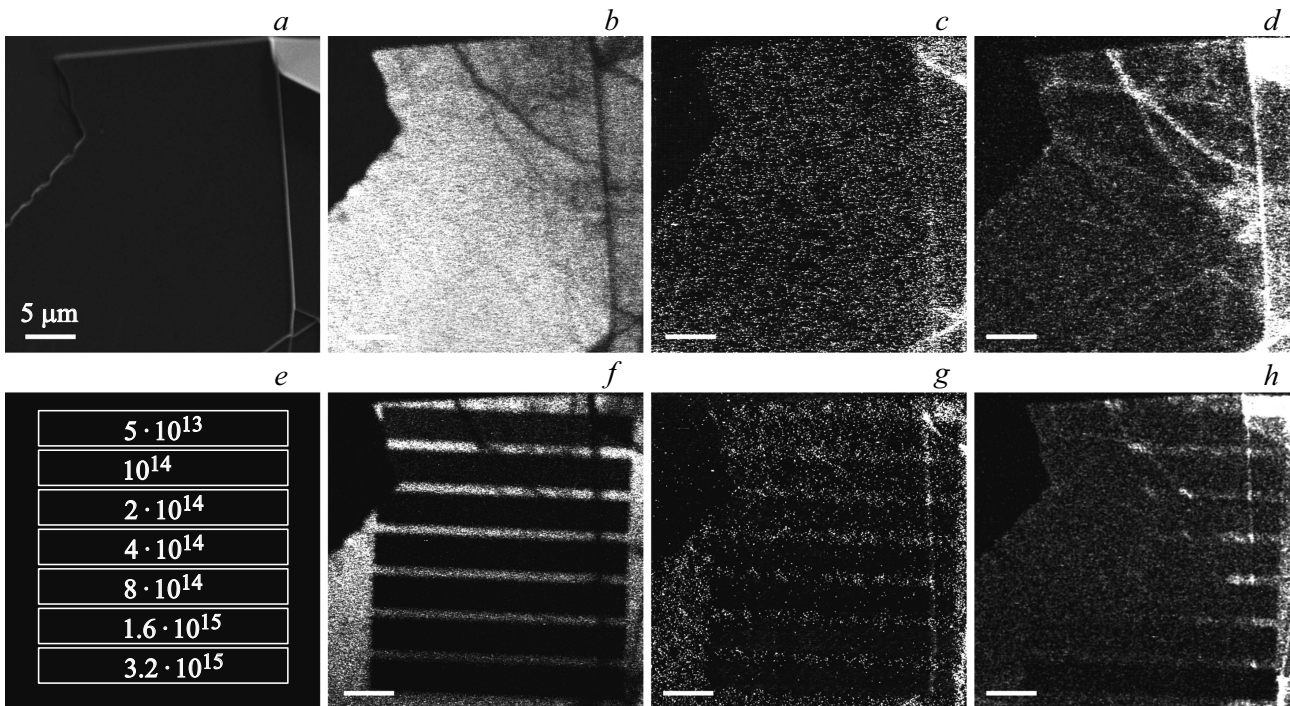


Figure 2. *a*) SEM image of the sample. *b–d*) CL maps of pristine sample at different wavelengths: *b* — 215 nm, *c* — 320 nm, *d* — 650 nm (bandpass filter). *e* — drawing of areas, irradiated with helium ions at different fluences. *f–h*) CL maps of the helium ion irradiated sample at different wavelengths: *f* — 215 nm, *g* — 320 nm, *h* — 650 nm (bandpass filter). Scale bar for all figures is 5 μm .

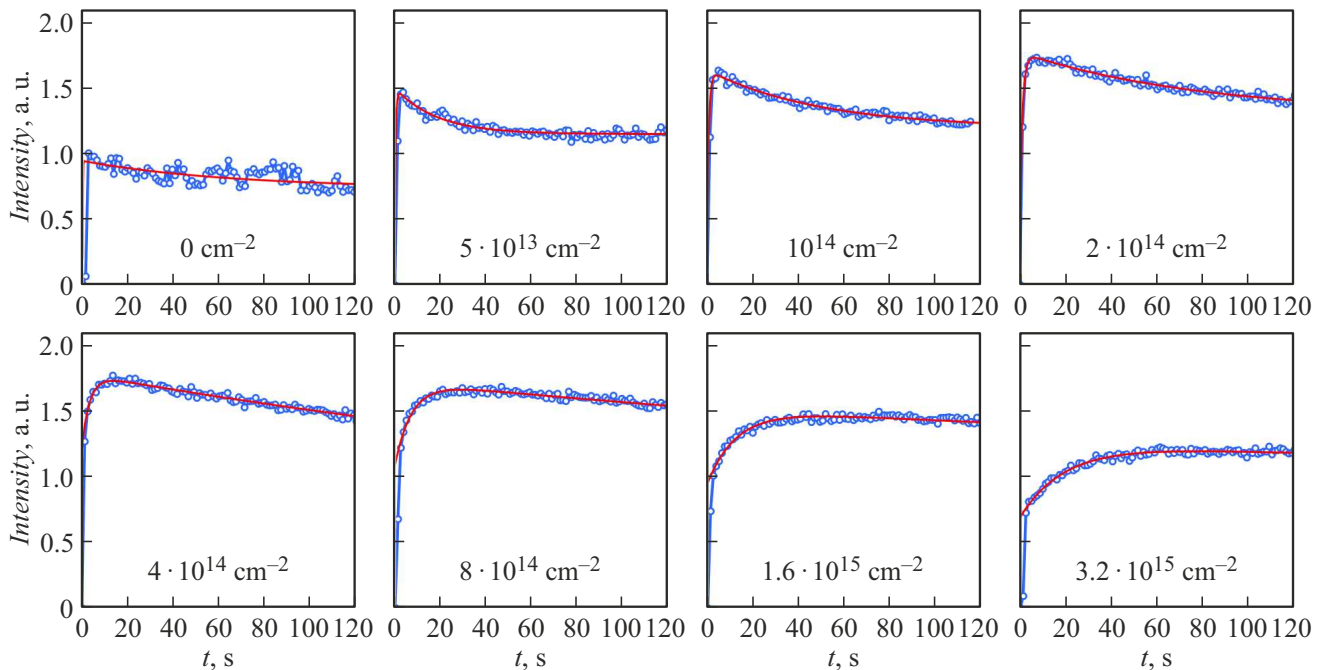


Figure 3. The dependence of the intensity of 640 nm band on electron irradiation time normalized to the intensity in pristine sample for different values of the helium ion irradiation fluence shown in the legend (zero fluence marks the pristine sample). Round dots and lines correspond to experimental data and the fit with equation (1) respectively.

resulted in decrease of the intensity of all CL bands. It can be explained by the formation of additional non-radiative recombination channel caused by ion induced defects that

give rise to the decrease of the lifetime of electron beam excited excess charge carriers. Similar effect was previously observed in [10,11,16].

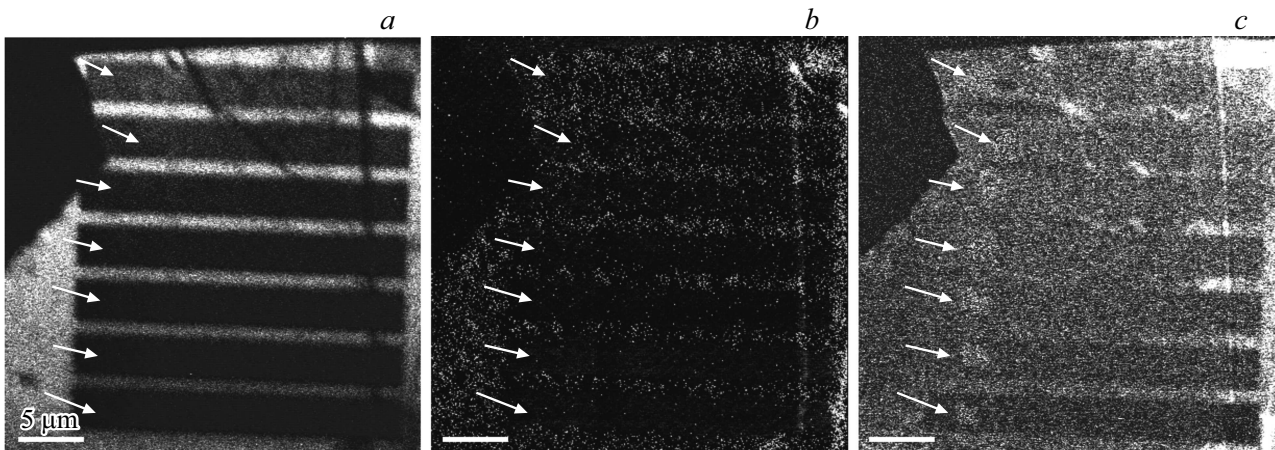


Figure 4. CL maps of the sample after the measurements of dependencies on electron irradiation time. *a* — 215 nm, *b* — 320 nm, *c* — 640 nm, arrows show areas, where the dependencies of intensity vs. time were measured from. Scale bar for all figures is 5 μm .

Time dependence of the intensity of 640 nm band under electron excitation can be approximated with a sum of exponential functions, where the first term represents the asymptotic rise, and the second term represents the decay:

$$I = a(1 - e^{-t/t_1}) + be^{-t/t_2}, \quad (1)$$

where I — CL intensity, t — electron irradiation time, a , b , t_1 and t_2 — fit parameters. The suggested expression describes well the dependencies of the intensity on time for all areas irradiated with various ion fluences. Respective curves are presented in Fig. 3 with lines for each experimental graph.

Time constants t_1 and t_2 for different helium ion irradiated areas of the sample are shown in Fig. 5 as a function of ion fluence.

A monotonous increase of both time constants with ion fluence allows one to suppose that ion induced defects formed under such impact play a significant role in the process of the variation of the concentration of luminescence centers. Since no increase of the intensity of 640 nm band was observed immediately after ion irradiation, one can assume that irradiation induced defects themselves are not the luminescence centers, however, they can be transformed into the such centers under electron irradiation that result in the intensity rise seen in the beginning of graphs in Fig. 3. The decrease of the intensity observed during prolonged electron irradiation, can be explained by the decrease of the concentration of luminescence centers caused by their transformation or/and by the formation of additional recombination channels decreasing the concentration of excess carriers. The version of the explanation that decrease of the intensity takes place as a result of hydrocarbon film deposition can be discarded, since the time constant corresponding to the intensity decrease depends on ion fluence monotonously, whereas the thickness of the layer deposited onto the surface does not correlate with ion fluence. To describe possible mechanisms that can lead to the observed variation of the intensity one should consider

the properties of the defects supposed to be centers of luminescence of the 1.9 eV band in more details.

The authors of [18–20] considered such luminescence centers to be boron dangling bonds, which might present at the edges or kinks of the layers, either appear as a result of bombardment with fast particles. According to the calculations, zero phonon transition energy of such center is 2.06 eV for bulk boron nitride without mechanical strain [18] and 2.02 eV for single layer [20], decreasing under mechanical strain. An increase of the intensity of 1.9 eV band at elongated structure features, observed in our work, agrees with this assumption since the sample morphology of such features can be considered as kinks formed during crystal exfoliation and transfer. Though ion irradiation of the sample creates significant number of vacancies, however, the electronic structure of several dangling bonds around a single vacancy substantially differs from the case described in [18–20] because of significant interaction of the nearest neighbors. To describe the dangling bonds the authors considered formation of voids, being clusters of four vacancies. Collision cascades under irradiation with light helium ions are practically absent, and the formation of isolated vacancies takes place, concentration of which, according to simulation with SRIM software [21], slowly increases with depth, and varies from 10^{21} cm^{-3} at the surface to $3 \cdot 10^{21} \text{ cm}^{-3}$ near the interface with the substrate, that is less than 6 at.% for the largest ion fluence used in our experiment. Therefore, formation of vacancies clusters seems to be unlikely directly under ion irradiation, but it might occur as a result of vacancy migration enhanced by recombination of excess carriers, excited with electron beam. Nowadays there are no data in literature on the possibility of such lustering of the vacancies, however, if the formation of the luminescence centers requires formation of clusters of the vacancies, with the ion fluence increase and, accordingly, with the increase of the vacancy concentration, the cluster formation process should be accelerated that contradicts our experimental

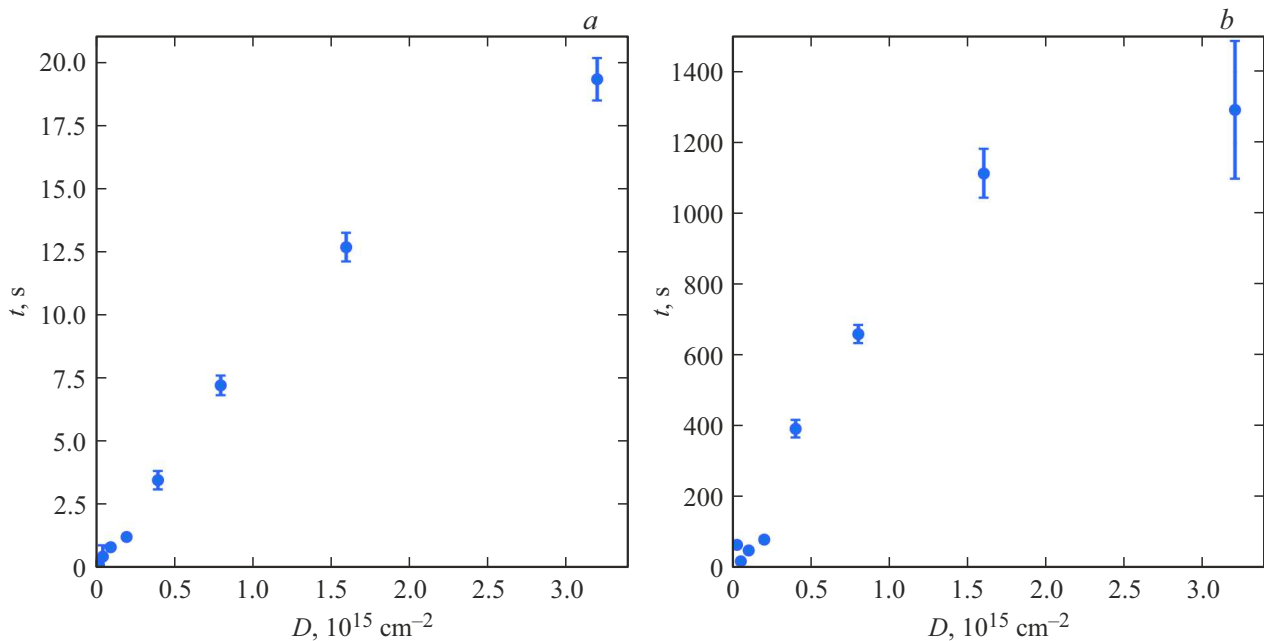


Figure 5. The dependences of the time constants, obtained from fit with eq. (1), on the helium ion fluence. a — t_1 , b — t_2 .

data on time constants. Moreover, in the case of such nature of the luminescence centers the explanation of the CL intensity decay during prolonged electron irradiation becomes not clear.

In refs. [11,22–24] the origin of the luminescence center 1.9 eV was ascribed to the complex of nitrogen vacancy with antisite defect $V_N N_B$. According to theoretical calculations, the energy of internal transition for such defect is 2.05 eV without strain and can either decrease or increase depending on the type and direction of structure strain. The probability of such defect formation under ion irradiation is rather small that agrees with the decrease of CL intensity observed in our experiment. The defects like $V_N N_B$ might be formed under subsequent electron beam irradiation from boron vacancy by a shift of the neighboring nitrogen atom to the boron site. Thus, if we consider $V_N N_B$ as a luminescence center of 1.9 eV band, we can suppose that boron vacancies, formed after ion impact under subsequent electron irradiation could be transformed to new luminescence centers, and that agrees with CL intensity rise observed in the beginning of experimental graphs. The observed subsequent decay of the intensity may be caused by reverse transformation of the centers to boron vacancies and/or due to the formation of new recombination centers decreasing of the concentration of excess charge carriers. Transformation of the antisite defect in A_3B_5 semiconductors is well-known process, for example, in gallium arsenide antisite defect As_{Ga} being electrically active center EL2 [25] can be transformed under external influence into gallium vacancy and interstitial arsenic. In hexagonal boron nitride similare transformation of nitrogen vacancy into antisite boron with boron vacancy $V_B B_N$ has been described theoretically in [26], and the energy barrier of such transition was estimated to be

of 2.86 eV. Assuming the same order of magnitude for energy barrier for the transition, which we are interested in, we can suppose that such process is highly unlikely at room temperature without external excitation, but it might be possible under electron beam excitation. Since the processes of the defect transformations are induced by excess charge carriers, the time constants of these processes are determined by the steady state concentration of excess carriers that decreases with helium ion fluence because of the increase of the concentration of recombination centers. The decrease of the concentration of excess charge carriers, in turn, results in slowing down all processes that agrees with experimentally observed increase of time constants (Fig. 5).

One more possible candidate suitable for the luminescence center in red part of the spectrum is a complex of the nitrogen vacancy and carbon impurity in boron site $V_N C_B$ [27–30]. The electron transition energy in such center according to calculations presented in [26,28] or [29] is 2.08 eV, 1.39 eV or 1.75 eV respectively and according to calculations presented in [29] it varies depending on applied mechanical strain. Using such configuration of the luminescence center, one might suppose that electron beam irradiation stimulates the formation of complexes of vacancies, formed under ion irradiation, and carbon impurities, which were in the sample before or were embedded during electron irradiation. However, 3.9 eV luminescence band is somehow carbon related [3,6], and its intensity in pristine sample was low, and no intensity increase was observed during electron irradiation. These indicate that carbon impurity concentration was sufficiently low and carbon embedding during electron irradiation was negligible, therefore, $V_N C_B$, as the origin of 1.9 eV

luminescence center is least experimentally confirmed from all other versions considered above.

Thus, among all models of luminescence centers, responsible for 1.9 eV luminescence band, $V_N N_B$ defect complex is the most approved with obtained experimental data on the variation of the intensity under electron irradiation of hexagonal boron nitride, previously irradiated with helium ions, and the model of dangling bonds describes the intensity increase at the kinks on h-BN surface. To clarify the nature of the luminescence centers, corresponding to 1.9 eV band, further investigations are required. Besides that, the presence of both types of defects in one sample cannot be excluded.

Conclusions

Our investigation of the effect of successive ion and electron irradiation on the intensity of various cathodoluminescence bands of hexagonal boron nitride shows that irradiation with focused helium ion beam results in formation of recombination centers with a high concentration, and subsequent electron irradiation resulted in increase of the concentration of luminescence centers, responsible for luminescence band at 640 nm (~ 1.9 eV). The maximum intensity of this band, achievable with electron irradiation, exceeds the intensity of the same band in non-irradiated material, and time constants of both rise and decay of the intensity increase with helium ion fluence that allows to use successive ion and electron irradiation to control the intensity of the luminescence. The most probable model describing such a process seems to be the formation of the luminescence centers by means of electron induced transformation of ion induced defects.

Acknowledgments

The research is supported by Russian Science Foundation, project № 23-22-00067, <https://rscf.ru/project/23-22-00067/>. Experimental results were obtained using the equipment of Interdisciplinary Resource Center for Nanotechnology of the Research Park of SPbSU. The authors are thankful to K. Watanabe and R. Taniguchi for the provided sample of hexagonal boron nitride and thankful to T.V. Sharov for his assistance with atomic force microscopy measurements.

References

- [1] I. Aharonovich, D. Englund, M. Toth. *Nature Photonics*, **10**, 631 (2016). DOI: 10.1038/NPHOTON.2016.186
- [2] N. Mizuochi, T. Makino, H. Kato, D. Takeuchi, M. Ogura, H. Okushi, M. Nothaft, P. Neumann, A. Gali, F. Jelezko, J. Wrachtrup, S. Yamasaki. *Nature Photonics*, **6** (2012). DOI: 10.1038/NPHOTON.2012.75
- [3] R. Bourrellier, S. Meuret, A. Tararan, O. Stéphan, M. Kociak, L.H.G. Tizei, A. Zobelli. *Nano Lett.*, **16**, 4317 (2016). DOI: 10.1021/acs.nanolett.6b01368
- [4] G. Cassabois, P. Valvin, B. Gil. *Nature Photonics*, **10**, 262 (2016). DOI: 10.1038/nphoton.2015.277
- [5] S. Castelletto, F.A. Inam, S. Sato, A. Boretti. *Beilstein J. Nanotechnol.* **11**, 740–769 (2020). DOI: 10.3762/bjnano.11.61
- [6] A. Vokhmintsev, I. Weinstein, D. Zamyatin. *Journal of Luminescence*, **208**, 363–370 (2019). DOI: 10.1016/j.jlumin.2018.12.036
- [7] N. Chejanovsky, M. Rezai, F. Paolucci, Y. Kim, T. Rendler, W. Rouabeh, F. Fávaro de Oliveira, P. Herlinger, A. Denisenko, S. Yang, I. Gerhardt, A. Finkler, J.H. Smet, J. Wrachtrup. *Nano Lett.*, **16**, 7037–7045 (2016). DOI: 10.1021/acs.nanolett.6b03268
- [8] J. Ziegler, R. Klais, A. Blaikie, D. Miller, V.R. Horowitz, B.J. Alemán. *Nano Lett.*, **19**, 2121–2127 (2019). DOI: 10.1021/acs.nanolett.9b00357
- [9] N.-J. Guo, W. Liu, Z.-P. Li, Y.-Z. Yang, S. Yu, Y. Meng, Z.-A. Wang, X.-D. Zeng, F.-F. Yan, Q. Li, J.-F. Wang, J.-S. Xu, Y.-T. Wang, J.-S. Tang, C.-F. Li, G.-C. Guo. *ACS Omega*, **7**, 1733–1739 (2022). DOI: 10.1021/acscomega.1c04564
- [10] Yu.V. Petrov, O.A. Gogina, O.F. Vyvenko, S. Kovalchuk, K. Bolotin, K. Watanabe, T. Taniguchi. *Technical Physics*, **92** (8), 984–989 (2022). DOI: 10.21883/TP.2022.08.54560.66-22
- [11] G. Grosso, H. Moon, B. Lienhard, S. Ali, D.K. Efetov, M.M. Furchi, P. Jarillo-Herrero, M.J. Ford, I. Aharonovich, D. Englund. *Nature Communications*, **8**, 705 (2017). DOI: 10.1038/s41467-017-00810-2
- [12] S. Choi, T. T. Tran, C. Elbadawi, C. Lobo, X. Wang, S. Juodkakis, G. Seniutinas, M. Toth, I. Aharonovich. *ACS Appl. Mater. Interfaces*, **8**, 29642 (2016). DOI: 10.1021/acsami.6b09875
- [13] F. Bianco, E. Corte, S.D. Tchernij, J. Forneris, F. Fabbri. *Nanomaterials* **13**, 739 (2023). DOI: 10.3390/nano13040739
- [14] H. Zhang, M. Lan, G. Tang, F. Chen, Z. Shu, F. Chend, M. Li. *J. Mater. Chem. C*, **7**, 12211 (2019). DOI: 10.1039/c9tc03695d
- [15] Yu.V. Petrov, O.F. Vyvenko, O.A. Gogina, K. Bolotin, S. Kovalchuk, K. Watanabe, T. Taniguchi. *J. Phys.: Conf. Series*. **2103** (1), 012065 (2021). DOI: 10.1088/1742-6596/2103/1/012065.
- [16] Yu.V. Petrov, O.F. Vyvenko, O.A. Gogina, T.V. Sharov, S. Kovalchuk, K. Bolotin. *Bulletin of the Russian Academy of Sciences: Physics*. **87**, 1455–1461 (2023). DOI: 10.3103/S1062873823703483
- [17] T. Taniguchi, K. Watanabe. *Journal of Crystal Growth*, **303**, 525–529 (2007). DOI: 10.1016/j.jcrysgro.2006.12.061
- [18] M.E. Turiansky, A. Alkauskas, L.C. Bassett, C.G. Van de Walle. *Phys. Rev. Lett.* **123**, 127401 (2019). DOI: 10.1103/PhysRevLett.123.127401
- [19] M.E. Turiansky, C.G. Van de Walle. *J. Appl. Phys.* **129**, 064301 (2021). DOI: 10.1063/5.0040780
- [20] M.E. Turiansky, C.G. Van de Walle. *2D Materials*, **8**, 024002 (2021). DOI: 10.1088/2053-1583/abe4bb
- [21] J.F. Ziegler, M.D. Ziegler, J.P. Biersack. *Nucl. Instr. Meth. Phys. Res. B*, **268**, 1818 (2010). DOI: 10.1016/j.nimb.2010.02.091
- [22] T.T. Tran, K. Bray, M.J. Ford, M. Toth, I. Aharonovich. *Nature Nanotechnology*, **11**, 37–42 (2015). DOI: 10.1038/NNANO.2015.242
- [23] F. Wu, T.J. Smart, J. Xu, Y. Ping. *Phys. Rev. B*, **100**, 081407 (2019). DOI: 10.1103/PhysRevB.100.081407

- [24] M. Abdi, J.-P. Chou, A. Gali, M.B. Plenio. ACS Photonics, **5**, 1967–1976 (2018). DOI: 10.1021/acsp Photonics.7b01442
- [25] M. Kaminska, E.R. Weber. Semiconductors and Semimetals. **38**, 59–89 (1993). DOI: 10.1016/S0080-8784(08)62798-2
- [26] T.B. Ngwenya, A.M. Ukpong, N. Chetty. Phys. Rev. B, **84**, 245425 (2011). DOI:10.1103/PhysRevB.84.245425
- [27] S.A. Tawfik, S. Ali, M. Fronzi, M. Kianinia, T.T. Tran, C. Stampfl, I. Aharonovich, M. Toth, M.J. Ford. Nanoscale, **9**, 13575–13582 (2017). DOI: 10.1039/C7NR04270A
- [28] A. Sajid, J.R. Reimers, M.J. Ford. Phys. Rev. B, **97**, 064101 (2018). DOI: 10.1103/PhysRevB.97.064101
- [29] A. Sajid, K.S. Thygesen. 2D Mater. **7**, 031007 (2020). DOI: 10.1088/2053-1583/ab8f61
- [30] M. Fischer, J.M. Caridad, A. Sajid, S. Ghaderzadeh, M. Ghorbani-Asl, L. Gammelgaard, P. Bøggild, K.S. Thygesen, A.V. Krasheninnikov, S. Xiao, M. Wubs, N. Stenger. Science Advances, **7**, eabe7138 (2021). DOI: 10.1126/sciadv.abe7138

Translated by Ego Translating